Transport in Porous Media **43:** 159–178, 2001.

Tidal Effects on Groundwater Motions

JOHN WANG and TING-KUEI TSAY
Department of Civil Engineering, National Taiwan University, Taipei 106, Taiwan

Abstract. Assuming a sharp interface between freshwater and seawater within a coastal aquifer, a theory is developed to account for the piezometric head movement of steady and unsteady components in terms of large- and small-time scales. Tidal fluctuations are simulated by a series of decomposed simple harmonic motions in time. Groundwater fluctuation induced by tidal motion is perturbed to the groundwater head of large-time scale. Ghyben–Herzberg formulation is applied for solutions of large-time scale and a unified formulation for various flows of small-time scale is derived (Strack, 1989). Approximate analytical solutions for amplitudes and phase lags of tidal groundwater motions and the freshwater–seawater interface for a coastal aquifer in a circular island are obtained. The induced fluctuation amplitude generally decays in distance with a parameter consisting of hydraulic conductivity, storage coefficient, thickness of aquifer and tidal period. The present approach can be applied to confined and unconfined aquifers, with only freshwater flows or interfacial flows. The theory is verified with some experimental results (Parlange, *et al.*, 1984; Nielson, 1990). It can also used to determine physical parameters of an aquifer by monitoring the groundwater fluctuations due to tidal motions (Carr and van der Kamp, 1969).

Key words: tides, freshwater-seawater interface, coastal aquifer.

1. Introduction

Groundwater is an important water resource, especially for islands bounded by seawater. Understanding of the groundwater movement will ensure its proper utilization. Due to the density difference, seawater intrudes underneath freshwater in the coastal aquifers. The intrusion of seawater increases the salinity concentration of the soil and water. Seawater intrusion may also be affected by the tidal motion. The fluctuating amplitude of the groundwater table decays with distance away from the coastline and the phase of fluctuation shifts as well. In 1963, Ferris indicated the relationship between conductivity and storage coefficient, mainly by measuring the water-surface fluctuation of observation wells and a river. Knight (1981) found that groundwater level is related to the root-mean-square of water level in the river and the fluctuation period. Moreover, Paralang *et al.* (1984) expanded the equations which describe responses of the groundwater level to that of a reservoir. However, the effect of density difference between seawater and groundwater was ignored. Although Nielsen (1990) noticed that the variation of soil structures after seawater intrusion, and geometric factor of inclined beach faces had influences on groundwater motions, no salinity distribution was discussed. The phenomenon of tidal effects on groundwater motions has been investigated quite intensively. How-

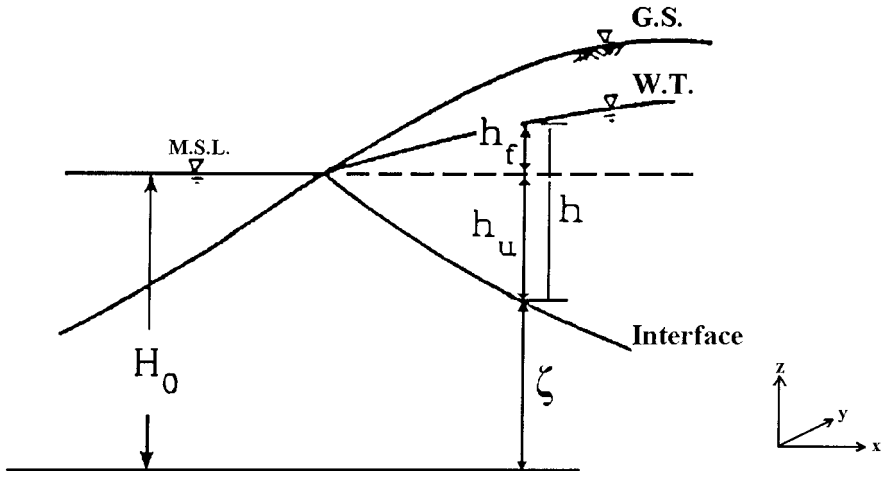

Figure 1. Definition of seawater intrusion.

ever, the theory for this problem has not been formulated. In this paper, a general mathematical approach for tidal effects on the groundwater motion is formulated. Tidal effects on the interface between freshwater and seawater are presented. An approximate analytical solution for tidal effects on coastal aquifer of a circular island is obtained. The numerical results of the proposed method are then compared with experimental results (Carr and van der Kamp, 1969; Parlange *et al.*, 1984; Nielsen, 1990).

2. Mathematical Formulation

Considering a column of unconfined aquifer of area dx dy with shallow interfacial flow, as shown in Figure 1, the equation of mass conservation can be written as:

$$\frac{\partial Q_x}{\partial x} + \frac{\partial Q_y}{\partial y} - N = -S\frac{\partial \phi}{\partial t}, \tag{1}$$

where Q(m^2/s) is the flowrate of the water column, the subscripts x and y represent quantities in x and y-direction, respectively; $\phi(m)$ is the piezometric head of groundwater; S (dimensionless) is the storage coefficient; and N(m/s) is rainfall intensity which reaches groundwater table. In reality, the time scale of groundwater movement is much larger than that of tidal fluctuation. It is therefore assumed that the discharge, Q, and piezometric head, ϕ, can be divided into two components, namely, components of large-time scale, Q_l and ϕ_l, and of small-time scale, Q_s and ϕ_s.

$$Q = Q_l + Q_s, \tag{2}$$

$$\phi = \phi_l + \phi_s. \tag{3}$$

The rainfall that reaches the groundwater table can be considered either in the large-time scale or in the small one based on the practical needs. To simplify

the analysis of tidal effects on groundwater motions and assuming that the annual average rainfall as the only available long-term freshwater resource on the island, rainfall intensity will be treated in the equation of large-time scale. The discharge, Q_{l}, and piezometric head, ϕ_{l} vary on a large-time scale (e.g. season or year) and may be assumed steady as compared to the small-time scale (e.g. day). On the other hand, Q_{s}, and ϕ_{s} are unsteady components when a small-time scale such as the tidal period is considered. By substitution of Equation (2) into Equation (1), groundwater motion can be described by the following two equations:

$$\frac{\partial Q_{\mathrm{l}x}}{\partial x} + \frac{\partial Q_{\mathrm{l}y}}{\partial y} - N = -S\frac{\partial \phi_{\mathrm{l}t}}{\partial t}, \tag{4}$$

$$\frac{\partial Q_{\mathrm{s}x}}{\partial x} + \frac{\partial Q_{\mathrm{s}y}}{\partial y} = -S\frac{\partial \phi_{\mathrm{s}t}}{\partial t}. \tag{5}$$

Equation (4) and (5) represent the mass conservation on large- and small-time scales, respectively. $\phi_{\mathrm{l}t}$ and $\phi_{\mathrm{s}t}$ are unsteady components of piezometric head. In the case of confined aquifers, no rainfall will reach the groundwater, therefore, Equations (1) and (4) are still applicable but N will be equal to zero and S has different physical meanings.

2.1. GOVERNING EQUATIONS FOR LARGE-TIME SCALE FLOW

To extend the applicability of Equation (4), a discharge potential (Strack, 1989) is introduced

$$Q_{\mathrm{l}x} = -\frac{\partial \Phi_{\mathrm{l}}}{\partial x}, \qquad Q_{\mathrm{l}y} = -\frac{\partial \Phi_{\mathrm{l}}}{\partial y} \tag{6}$$

and

$$\Phi_{\mathrm{l}} = \tfrac{1}{2}kc_1\phi_{\mathrm{l}}^2 + kc_2\phi_{\mathrm{l}} + c_3 \tag{7}$$

in which

$$c_1 = 1, \qquad c_2 = 0, \qquad c_3 = 0$$

for unconfined freshwater flows

$$c_1 = 0, \qquad c_2 = H, \qquad c_3 = -\tfrac{1}{2}kH^2$$

for confined freshwater flows

$$c_1 = \alpha - 1, \quad c_2 = -\alpha H_0 + H, \quad c_3 = \frac{k}{2(\alpha-1)}(\alpha^2 H_0^2 - (\alpha-1)H^2)$$

for confined interfacial flows, and

$$c_1 = \alpha, \quad c_2 = -\alpha H_0, \quad c_3 = \frac{1}{2}k\left(3 - \alpha + \frac{1}{\alpha - 1}\right)H_0^2$$

for unconfined interfacial flows, where: k is hydraulic conductivity; $\alpha = \rho_b/(\rho_b - \rho_f)$ and ρ is fluid density; and subscripts of f and b refer to the freshwater and seawater, respectively; H_0 is the still sea level height measured from a specified datum, and H is the thickness of confined aquifer.

Substituting Equations (6) and (7) into Equation (4)

$$\frac{\partial^2 \Phi_l}{\partial x^2} + \frac{\partial^2 \Phi_l}{\partial y^2} + N = \frac{S}{k\bar{\phi}_f}\frac{\partial \Phi_l}{\partial t}, \tag{8}$$

where, $\bar{\phi}_f = c_1\phi_l + c_2$. In small-time scale, the discharge potential of large-time scale, Φ_l, is slowly-varying and can be viewed as steady.

$$\nabla^2 \Phi_l = -N \tag{9}$$

for unconfined aquifers and

$$\nabla^2 \Phi_l = 0 \tag{10}$$

for confined aquifers.

Equations (9) and (10) can be applied to either pure freshwater or interfacial flows. The difference between various types of flow appears only in the definition of the potential discharge defined in Equation (7).

2.2. GOVERNING EQUATIONS FOR SMALL-TIME SCALE FLOW

A coastal unconfined aquifer of freshwater is considered as shown in Figure 1. For the case of confined aquifers, an impermeable boundary will replace the phreatic surface. In both cases, the freshwater and seawater piezometric heads, ϕ_f, and ϕ_b, are defined as:

$$\phi_f = \frac{p_f}{\gamma_f} + z_f \tag{11}$$

$$\phi_b = \frac{p_b}{\gamma_b} + z_b \tag{12}$$

where z is elevation, p is pressure, and γ is specific weight. Subscripts f and b refer to freshwater and seawater regions, respectively. Along the interface, $z = \zeta$, the pressure and elevation are continuous, such that

$$\gamma_b\phi_b - \gamma_f\phi_f = (\gamma_b - \gamma_f)\zeta. \tag{13}$$

Total piezometric head and free surface elevation can be separated into large-and small-time components

$$\phi_b = \phi_{bl} + \phi_{bs}, \tag{14}$$

$$\phi_f = \phi_{fl} + \phi_{fs}, \tag{15}$$

$$\zeta = \zeta_l + \zeta_s, \tag{16}$$

where ϕ_{bl}, ϕ_{fl}, and ζ_l are components in large-time scale; ϕ_{bs}, ϕ_{fs} and ζ_s are unsteady (i.e. small-time scale) components. Substituting Equations (14)–(16) into Equation (13), and assuming that the fluctuation of groundwater in small-time scale is a perturbation of groundwater movement in large-time scale, the steady and unsteady parts can be rewritten as

$$\gamma_b \phi_{bl} - \gamma_f \phi_{fl} = (\gamma_b - \gamma_f)\zeta_l, \tag{17}$$

$$\gamma_b \phi_{bs} - \gamma_f \phi_{fs} = (\gamma_b - \gamma_f)\zeta_s. \tag{18}$$

It should be noted that Equation (17) is identical to the well-known Ghyben-Herzberg equation (Strack, 1989). And Equation (18) can be rewritten as

$$\phi_{bs} = \left(\frac{\gamma_f}{\gamma_b}\right)\phi_{fs} + \frac{(\gamma_b - \gamma_f)}{\gamma_b}\zeta_s. \tag{19}$$

For practical applications $\rho_b = 1030\,\mathrm{kg/m^3}$, and $\rho_f = 1000\,\mathrm{kg/m^3}$, The second term of Equation (19) is very small as compared to the first one and may thus be neglected. Therefore,

$$\phi_{bs} \cong \left(\frac{\gamma_f}{\gamma_b}\right)\phi_{fs}. \tag{20}$$

Using Darcy's law, the total horizontal discharge in both the freshwater and seawater regions can be expressed as

$$Q_x = -k_f h \frac{\partial \phi_f}{\partial x} - k_s \zeta \frac{\partial \phi_b}{\partial x}, \tag{21}$$

$$Q_y = -k_f h \frac{\partial \phi_f}{\partial y} - k_s \zeta \frac{\partial \phi_b}{\partial y}, \tag{22}$$

where k_f and k_s are the hydraulic conductivities in freshwater and seawater regions, respectively, and h the thickness of freshwater layer. The hydraulic conductivity k can be expressed as $k = k^* g/\nu$ (Nutting, 1930), where k^*, the intrinsic permeability, depends solely on the property of solid matrix; and ν is the kinematic viscosity of the fluid. Under the same solid matrix of porous media, $k_f = \nu_s k_s/\nu_f$, Equations (21) and (22) become

$$Q_x = -k_f \left(h \frac{\partial \phi_f}{\partial x} + \frac{\zeta \nu_f}{\nu_s}\frac{\partial \phi_b}{\partial x}\right) \tag{23}$$

$$Q_y = -k_f \left(h \frac{\partial \phi_f}{\partial y} + \frac{\zeta \nu_f}{\nu_s}\frac{\partial \phi_b}{\partial y}\right). \tag{24}$$

Assuming that the component of the large-time scale varies slowly in x and y-direction, and substituting Equations (14), (15), and (20) into Equations (23) and

(24), with $h = \phi_f - \zeta$ for unconfined aquifers; $h = H - \zeta$ for confined aquifers

$$Q_{sx} = -k_f \frac{\partial \phi_{fs}}{\partial x}(\epsilon\zeta + \phi_w) \tag{25}$$

$$Q_{sy} = -k_f \frac{\partial \phi_{fs}}{\partial y}(\epsilon\zeta + \phi_w) \tag{26}$$

where $\epsilon = (\gamma_f/\gamma_b)(\nu_f/\nu_s) - 1$ and $\phi_w = \phi_f$ for unconfined aquifers; and $\phi_w = cH$, $c = \gamma_f/1.046\gamma_b$ for confined aquifers.

With substitution of Equations (25) and (26), Equation (5) can be rewritten as

$$\frac{\partial}{\partial x}\left[(\epsilon\zeta + \phi_w)\frac{\partial \phi_{fs}}{\partial x}\right] + \frac{\partial}{\partial y}\left[(\epsilon\zeta + \phi_w)\frac{\partial \phi_{fs}}{\partial y}\right] = \frac{S}{k}\frac{\partial \phi_{fs}}{\partial t}. \tag{27}$$

For aquifers of pure freshwater, i.e. $\gamma_f = \gamma_b$ and $\nu_f = \nu_s$, the parameter ϵ is equal to zero. For shallow interfacial flows, by taking ρ_b as 1030 kg/m^3 and ρ_f as 1000 kg/m^3, with $\nu_f = 1.01 \times 10^{-6}$(m^2/s), and $\nu_s = 1.06 \times 10^{-6}$(m^2/s), at 20°C, ϵ in Equation (27) is thus equal to 0.028. Even at the intrusion boundary where the freshwater is the thinnest, the ratio of $\epsilon\zeta$ to ϕ_w is only 0.028. Therefore, it is reasonable to further simplify Equation (27) as follows to describe one-phase and two-phase flows

$$\frac{\partial}{\partial x}\left(\phi_w \frac{\partial \phi_{fs}}{\partial x}\right) + \frac{\partial}{\partial y}\left(\phi_w \frac{\partial \phi_{fs}}{\partial y}\right) = \frac{S}{k}\frac{\partial \phi_{fs}}{\partial t}, \tag{28}$$

with $\phi_w = \phi_f$ and $S = S_u$ for unconfined aquifers, and $\phi_w = H$ and $S = S_c = \gamma H(m_v + n\beta_\omega)$ for confined aquifers. S_u and S_c are the storage coefficient of unconfined and confined aquifers, respectively. m_v is the coefficient of volume compressibility; n is the porosity, and β_ω the compressibility of water. Recalling that ϕ_s is much less than ϕ_l, thus ϕ_f may be approximated by ϕ_l.

The fluctuation of tides may be represented by linear composition of simple harmonic motions in time, t. Without losing generality, one component of tides is considered

$$\phi_{fs} = \phi' e^{-i\omega t}, \tag{29}$$

where ϕ' is the response amplitude of unsteady piezometric head, ω is the radian frequencies of tides and $i = \sqrt{-1}$ is a pure imaginary number.

By substitution of Equation (29), Equation (28) is reduced to

$$\frac{\partial}{\partial x}\left(\phi_w \frac{\partial \phi'}{\partial x}\right) + \frac{\partial}{\partial y}\left(\phi_w \frac{\partial \phi'}{\partial y}\right) = \frac{-i\omega S}{k}\phi'. \tag{30}$$

To investigate the tidal effects on the groundwater motion, ϕ' can be calculated from Equations (30) and ϕ_w from Equation (9) or (10). Thus, the total piezometric head can be obtained by superposition of the piezometric components of small- and large-time scales.

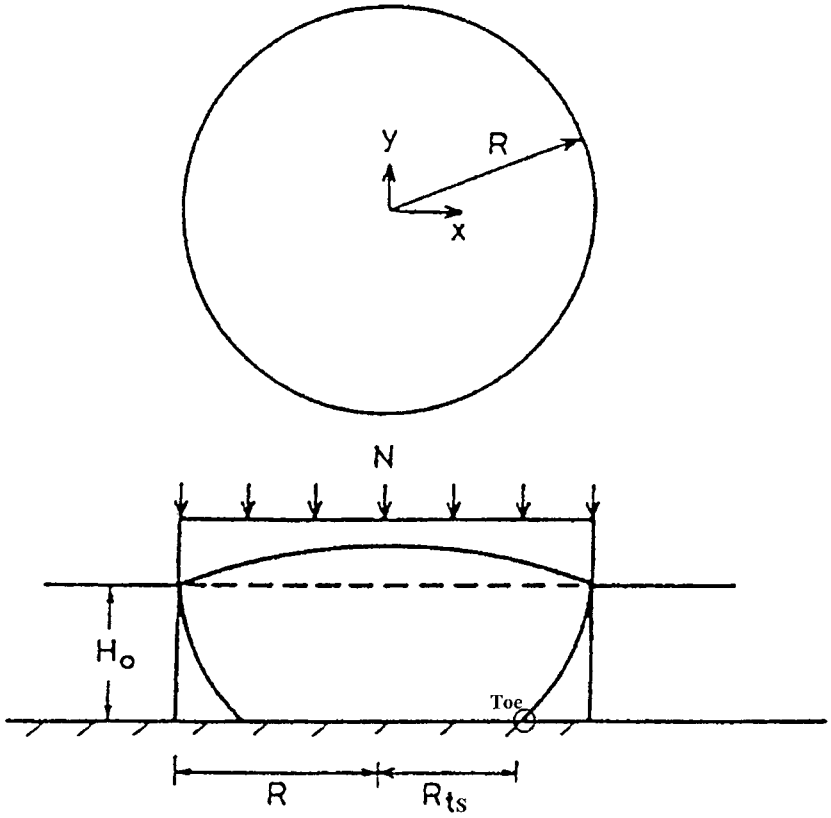

Figure 2. A circular island in the sea.

3. Approximate Analytical Solutions

3.1. SHALLOW UNCONFINED INTERFACIAL FLOW FOR A CIRCULAR ISLAND

In analyzing the case of shallow unconfined interfacial flow for a circular island with radius, R, piezometric heads of large and small-time scales are estimated respectively (Figure 2). Then the two components are added to achieve the total piezometric head.

To evaluate large-time piezometric head, ϕ_l, Equation (9) is considered, with boundary conditions of no-flux at the center of the island and constant head of the mean seawater elevation, H_0, along the coast, $r = R$. The solutions have been obtained in polar coordinate (Strack, 1989).

$$\Phi_l = \frac{1}{4}N(R^2 - r^2) + \frac{\rho_b}{2\rho_f}k_f {H_0}^2, \tag{31}$$

$$\phi_l = H_0 + \sqrt{\frac{N(R^2 - r^2)}{2k\alpha}}. \tag{32}$$

The large-time scale component of interface elevation is

$$\zeta_1 = H_0 - \sqrt{\frac{\rho_f^2 N(R^2 - r^2)}{2k\rho_b(\rho_b - \rho_f)}}. \tag{33}$$

At the toe of seawater intrusion, $\zeta_1 = 0$. The location of the toe, $r = R_{ts}$, can then be determined as

$$R_{ts} = R\sqrt{1 - \frac{2\rho_b k H_0^2(\rho_b - \rho_f)}{NR^2\rho_f^2}}. \tag{34}$$

There exists a minimal rainfall intensity to have real roots of Equation (34). Otherwise, the freshwater will be suspended in the form of a lens on top of seawater.

$$N \geqslant \frac{2\rho_b k H_0^2(\rho_b - \rho_f)}{R^2\rho_f^2}. \tag{35}$$

To investigate the tidal effects, one can further assume that the large-time component of piezometric head, ϕ_w , is a slowly-varying function of distance and may be performed by a representative quantity, for example, the averaged ϕ_w from the integration of Equation (32), or $\phi_w = 0.5(H_0 + H_1)$, where H_1 is the height of the water at the center of island. This method is similar to 'the second type' linearization that takes a regional average quantity to linearize a nonlinear equation (Brutsaert and Ibrahim, 1966; Bear, 1972). Furthermore, for one-dimensional case, the average height of groundwater H has been discussed by Knight (1981). The result of $h_\infty^2 = \langle h_1^2 \rangle$ was introduced, where h_1 is the water surface height at $x = 0$ and $\langle\rangle$ means the averaged value in periodic time interval. Knight (1981) did not consider the Dupuit-Forchheimer assumption.

To obtain the piezometric head of small-time scale, let

$$a^2 = \frac{i\omega S}{k\phi_w}, \quad a = b(1+i), \quad b = \sqrt{\frac{\omega S}{2k\phi_w}}. \tag{36}$$

Equation (30) can be rewritten as

$$\frac{\partial^2\phi'}{\partial x^2} + \frac{\partial^2\phi'}{\partial y^2} = -a^2\phi'. \tag{37}$$

Equation (37) is subject to conditions that ϕ' is finite at the geometric center and the tidal amplitude $\phi' = \phi_0'$ at the boundary of the circular island. By using the method of separation of variables, and applying the orthogonality condition of sinusoidal functions, one can obtain

$$\phi' = \phi_0' \frac{J_0(\mathrm{ar})}{J_0(aR)}. \tag{38}$$

Thus, the fluctuation of groundwater piezometric head can be approximated as:

$$\phi_{\mathrm{f}} = \phi_{\mathrm{fl}} + \phi_{\mathrm{fs}} = \phi_{\mathrm{fl}} + \sum_{j=1}^{n} (\phi_0')_j \frac{J_0(a_j r)}{J_0(a_j R)} e^{-i\omega_j t} \tag{39}$$

when n components of tides are considered.

3.2. ONE-DIMENSIONAL SHALLOW UNCONFINED FRESHWATER FLOWS

Due to the availability of experimental measurements, the mathematical formulation developed in previous section is simplified to the one-dimensional case to verify the present theory. When an unconfined aquifer in a rectangular tank with a finite length L is considered, the governing equation can be rewritten as

$$\frac{\mathrm{d}^2 \Phi_{\mathrm{l}}}{\mathrm{d}x^2} + N = 0 \tag{40}$$

Assuming that $N = 0$, and the boundary conditions are: $\Phi_{\mathrm{l}} = \frac{1}{2} k {\phi_{\mathrm{l}o}}^2$ at $x = 0$ and $\mathrm{d}\Phi_{\mathrm{l}}/\mathrm{d}x = 0$ at a finite length, $x = L$. It can be shown that

$$\Phi_l = \tfrac{1}{2} k {\phi_{\mathrm{l}o}}^2, \tag{41}$$

and from Equation (37), the response of tidal effects is governed by

$$\frac{\mathrm{d}^2 \phi'}{\mathrm{d}x^2} = -a^2 \phi', \tag{42}$$

with boundary conditions: $\phi' = \phi_0'$ at $x = 0$ and $\mathrm{d}\phi_{\mathrm{l}}/\mathrm{d}x = 0$ at $x = L$. The solution of small-time piezometric component can be obtained from Equation (42):

$$\begin{aligned} \phi_{\mathrm{fs}} \;=\; & \frac{\phi_0' e^{-i\omega t}}{\cosh\, 2bL + \cos\, bL - \sin\, bL} \times \\ & \times\, \cos[bL(1-i)] \cos[b(L-x)(1+i)]. \end{aligned} \tag{43}$$

Note that only the real part of Equation (43) has physical meaning.

3.3. ONE-DIMENSIONAL SHALLOW INTERFACIAL FLOWS

In this section, analytical solutions for shallow interfacial flows in one-dimensional cases are presented. Consider a well that is located at a distance x_1 from $x = 0$, and the amplitude of small-time piezometric head in the well is measured as ϕ_0'. Location $x = 0$ is defined as the intersectional point of mean seawater level and the beach. When the boundary in the landward direction is not limited, the boundary condition can be specified as $\phi' \to 0$ when $x \to \infty$. In this case, the analytical solution becomes

$$\phi' = \phi_0' e^{-\mathrm{b}(x - x_1)} e^{i\mathrm{b}(x - x_1)}. \tag{44}$$

The piezometric head of small-time scale can be expressed as

$$\phi_{\mathrm{fs}} = \phi_0' e^{-\mathrm{b}(x - x_1)} e^{i(bx - \omega t - bx_1)}. \tag{45}$$

For physical small-time groundwater fluctuations, the real part of (45) is taken as

$$\phi_{\mathrm{fs}} = \phi_0' e^{-b(x-x_1)} \cos(bx - \omega t - bx_1) \tag{46}$$

4. Numerical Examples

4.1. SHALLOW UNCONFINED INTERFACIAL FLOW OF A CIRCULAR ISLAND

A circular island with radius, R, of 5 km is used as a numerical example to illustrate tidal effects on a coastal aquifer. The aquifer is assumed to be unconfined with a hydraulic conductivity, $k = 0.01$ m/s, and a storage coefficient, $S = 0.25$. The island has an average net rainfall intensity, $N = 8.0 \times 10^{-8}$ m/s and a tidal period that is approximately equal to 13 h. Typical values of densities for seawater, 1030 kg/m^3, and freshwater, 1000 kg/m^3, are used. The mean seawater surface elevation H_0 is assumed to be 50 m above a reference datum. The groundwater table is computed with Equation (31) and shown in Figure 3. The apex of the water surface curve is at the center of the island and is set at 51.7 m above the datum. The gradient of the water surface is rather small (about 0.034). Therefore, ϕ_{fl} is reasonably considered as slightly varying in x- and y-directions. The groundwater table and the interface elevation in terms of normalized radius r/R are shown in Figure 4, which

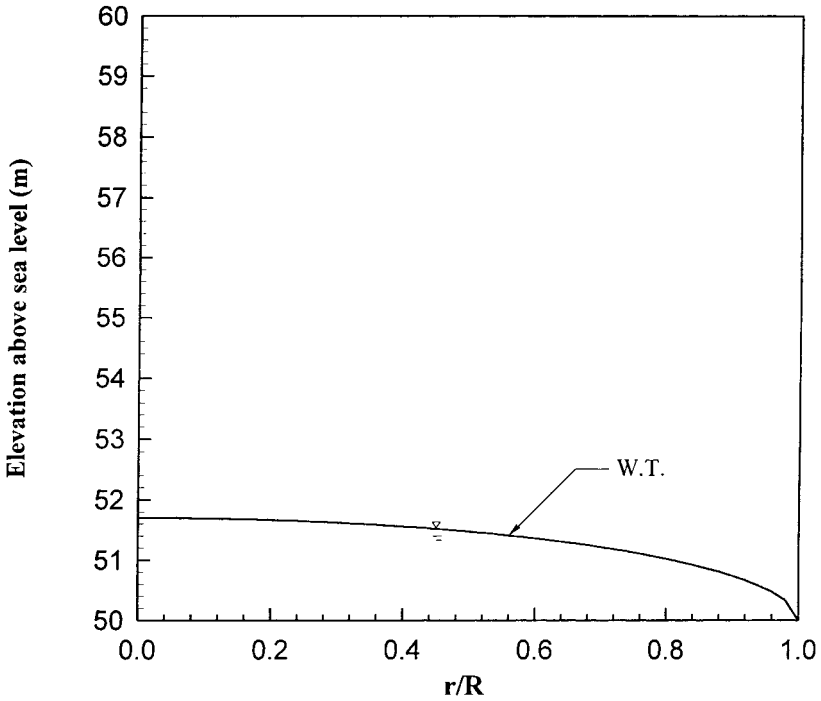

Figure 3. Distribution of freesurface elevation for a circular coastal aquifer.

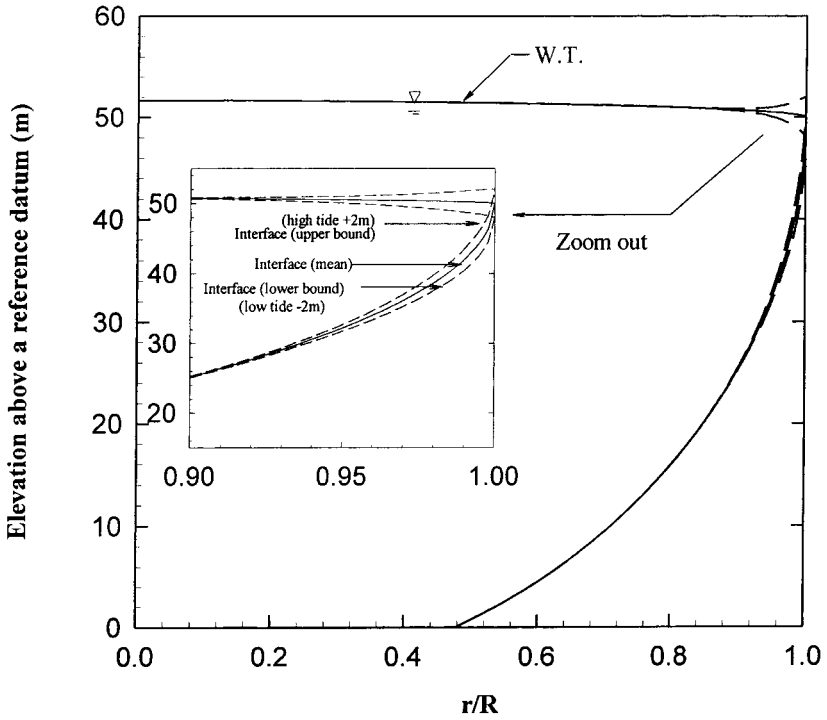

Figure 4. Profile of freshwater–seawater interface for a circular coastal aquifer.

is computed from Equations (32) and (33). It is also demonstrated in Figure 4 that the thickness of the layer with variable density may be approximated by perturbing the groundwater fluctuation induced by a short-time scale tide to the interfacial elevation of large-time scale. A tide of 2 m amplitude and 13 h period is assumed and seawater intrusion into the coastal unconfined aquifer induced by the tidal effect is calculated. The envelopes of free surface and the corresponding interfaces are shown in the inset of Figure 4. The influence of tide to the groundwater decays fast from $r/R = 1$ to $r/R = 0.9$. In reality, the water density within the envelope of interface will result in variable density distribution.

Seawater intrudes to the point at a radius of 2385 m. The normalized amplitudes of small-time scale fluctuations at different locations within the range of $0.78R$ to R due to tidal fluctuation are shown in Figure 5, which is obtained from Equation (38) with the second type linearization of ϕ_w, for different tidal periods. The tidal effects decay faster for smaller tidal periods. It can be expected that for much smaller waves, such as wind waves, the effects of wave fluctuations are bounded in a very small distance from the shoreline. For example, the normalized amplitudes for tides of 1.625 h have decayed to 7%, 0.5%, and 0.03% at distances of $r/R = 0.968$, 0.952, and 0.902, respectively. On the other hands, for tides with a period of 13 h, the normalized amplitudes have decayed to 40%, 15% and 6% at the same locations, respectively.

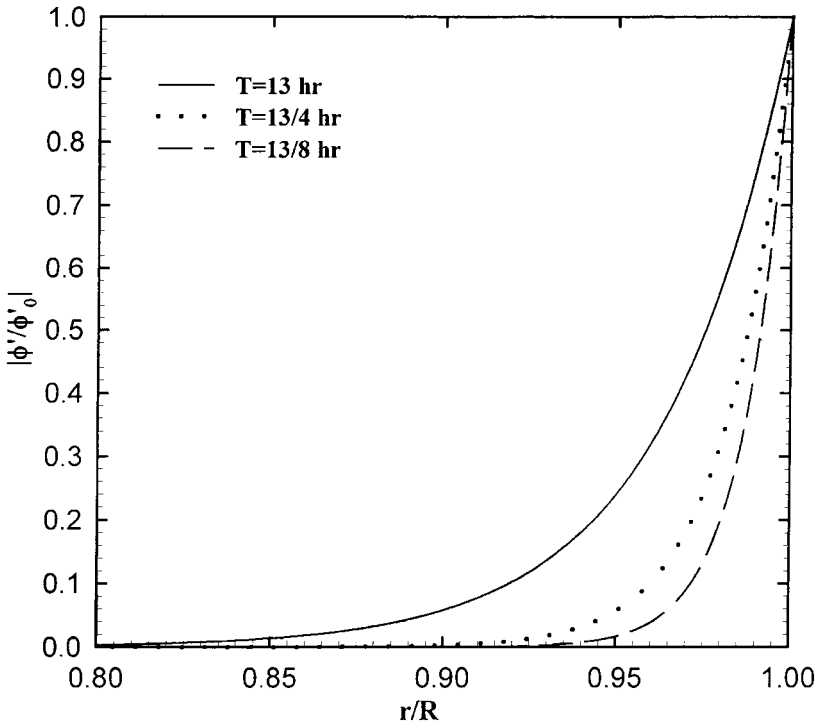

Figure 5. Distribution of normalized amplitudes in the radial direction of a circular coastal aquifer (R = 5 km).

The normalized groundwater fluctuations of small-time scale for a tidal period, $T = 13$ h at $r/R = 0.902$, 0.952, 0.968, and 1, are shown in Figure 6 (computed from Equation (38)). The amplitude of groundwater fluctuation decays with distance from the shoreline. The smaller the period, the higher the phase shift at the same distance. For harmonic motions, the phase shifts linearly with distance from the coastline. At a specific location, smaller tidal periods have larger phase-shifts.

4.2. ONE-DIMENSIONAL SHALLOW UNCONFINED FRESHWATER FLOWS

An experiment was carried out by Parlange *et al.* (1984) in a glass tank filled with gravels, 0.5 cm in diameter. The gravel was in contact with the reservoir as shown in Figure 7. Glycerol was used as a working fluid and the room temperature was kept constant at 27.4°C. The liquid in the reservoir was forced to oscillate by the vertical motion of a piston eccentrically connected to a wheel moving at a constant angular speed. The definition of the liquid surface is slightly ambiguous since some capillary rise may occur at the surface. The bottom of the menisci in the pores were taken to define the water surface. The average elevation of free-surface, $\tilde{\phi}$, was measured as 28.856 cm. The oscillation in the reservoir, $x = 0$, is not truly a harmonic motion of single period, Figure 8. For simplicity, a simple har-

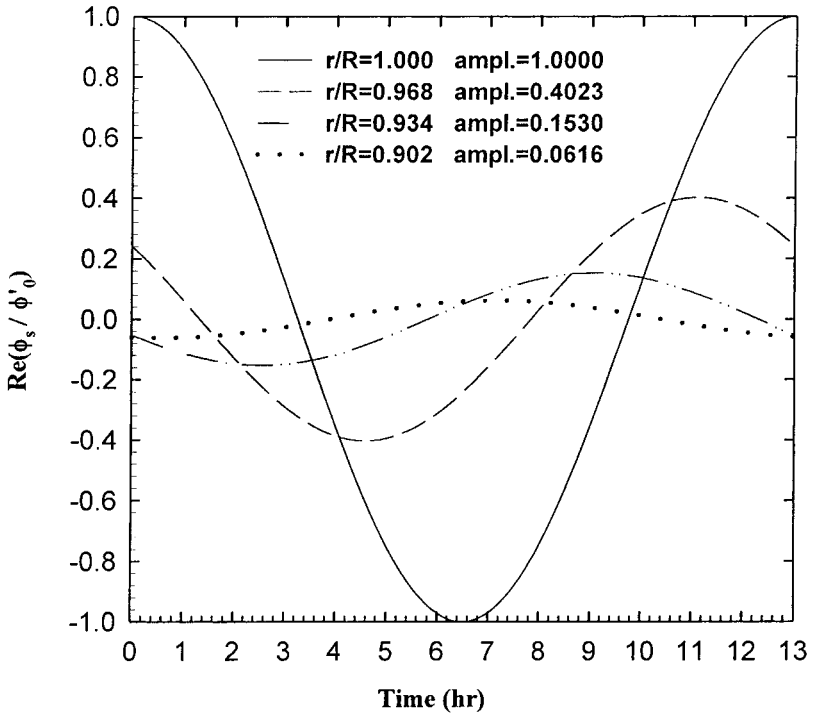

Figure 6. Normalized fluctuations of small-time scale at different locations, r/R = 1, 0.968, 0.934, 0.902 km, of a circular coastal aquifer for R = 5 km and T = 13 h.

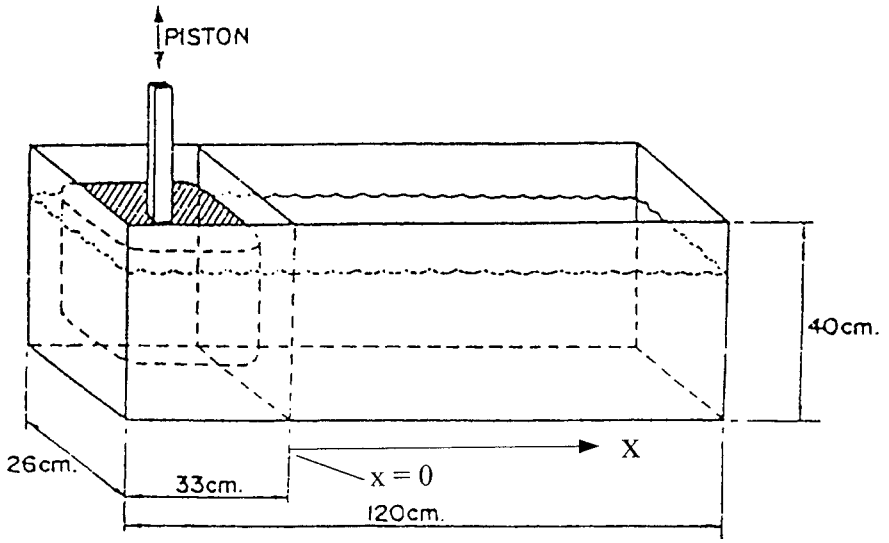

Figure 7. Diagrammatic representation of the oscillating reservoir experiment (after Parlange *et al.*, 1984).

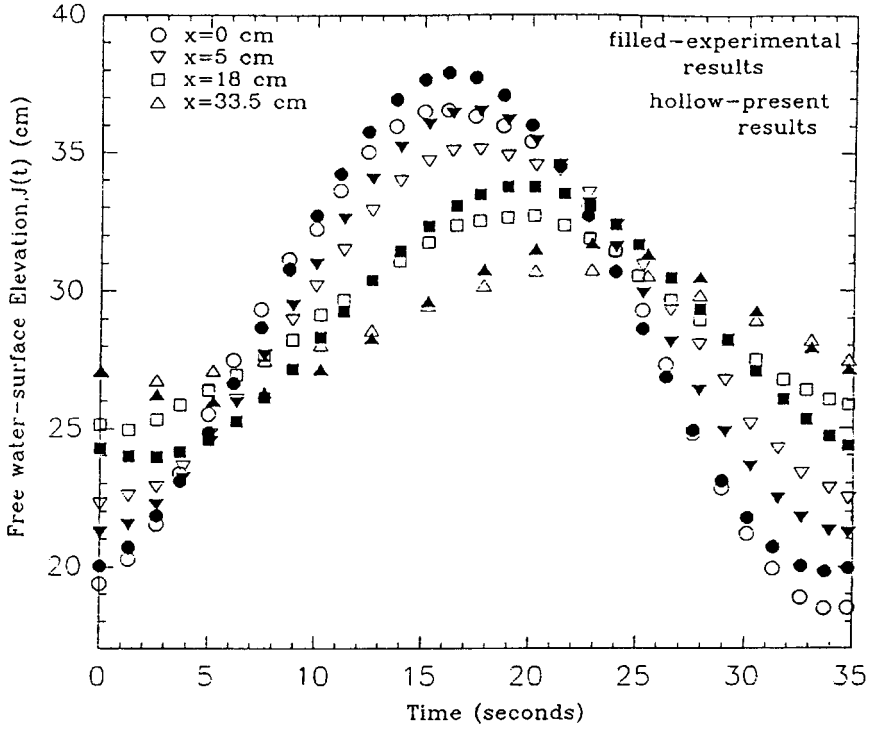

Figure 8. Comparisons of the computed and measured free-surface.

monic motion of period, $T = 35$ s is assumed in this verification. The comparison between the experimental results and the analytic solutions, Equation (43) is shown in Figure 8. Free-surface elevations at $x = 0$, 5, 18 and 33.5 cm are plotted versus time. The agreement between the computed and measured elevations is good, though the former result into smaller amplitudes. The phase lags of tidally-induced groundwater oscillation increase with distance from the reservoir. Differences in amplitude and period between experimental data and theoretical ones at the reservoir may result in some discrepancies between the computed and experimental elevations. To obtain better approximation, more than one tidal period should be used to represent the water fluctuations in the reservoir.

4.3. ONE-DIMENSIONAL SHALLOW UNCONFINED INTERFACIAL FLOWS

A one-dimensional, shallow unconfined interfacial flow was illustrated by Nielsen's experiment (1990). Nielsen's field experimental data was measured on April 18–19, 1989 every half an hour for 25 h on Barrenjoey Beach north of Sydney, Australia. Measurements were taken in 11 stilling wells placed at 2.5 m intervals along a section normal to the beach. Well No.7 (sand level 0.64 m) was the first well landward from the high water mark (sand level 0.516 m). The wind waves arriving at the beach had an estimated height of 5–10 cm. Groundwater in well No. 11 is

Table I. Constants of spectrum analysis for groundwater observations, Barrenjoey Beach, April 18–19, 1989

Well No.	5	6	7	8	9	10	11
$x(m)$	1.600	4.100	6.600	9.100	11.600	14.100	16.600
$\phi_0^{'}(m)$	0.162	0.208	0.248	0.262	0.270	0.282	0.290
$\phi_1^{'}(m)$	0.041	0.040	0.038	0.032	0.025	0.020	0.019
$\phi_2^{'}(m)$	0.265	0.228	0.193	0.139	0.107	0.086	0.075
$\phi_3^{'}(m)$	0.027	0.020	0.010	0.005	0.007	0.009	0.008
$\phi_4^{'}(m)$	0.084	0.066	0.055	0.023	0.016	0.016	0.011
φ_1	−1.886	−2.229	−2.075	−2.323	−2.406	−2.360	−2.342
φ_2	−2.705	−2.995	−3.030	3.106	2.887	2.794	2.729
φ_3	1.050	0.869	0.949	0.062	−0.246	−0.527	−0.643
φ_4	1.086	0.797	0.729	0.290	−0.159	−0.374	−0.539

lagging approximately one hour behind well No.7. However, without considering the effects of a sloping beach, a seepage face, or the wave actions on the beach, only experimental data of inland stilling wells were taken, namely, wells No. 5–9 and 11.

Using the spectrum analysis method with fast Fourier transform (FFT), by setting a threshold-value of the amplitudes, five significant components ($T_0 = \infty$, $T_1 = 24.5$, $T_2 = 12.25$, $T_3 = 8.17$, and $T_4 = 6.13$ h) are determined and shown in Table I. The first component of amplitudes indicates the average groundwater table. Thus, Equation (46) can be rewritten

$$\phi_{\mathrm{fs}} = \sum_{i=1}^{i=4} \phi'_{0i} e^{-b(x-x_1)} \cos(bx - \omega_i t - bx_1). \tag{47}$$

The reconstructions of groundwater free-surface fluctuation at wells No. 6–11 by Equation (47) are shown in Figure 9. A very good result is obtained. From Equation (47), it is observed that both the amplitude decaying rate and phase lag increase in proportion to bx. Thus, for each tidal periodic component, plots of amplitudes and phase lag against distance will yield the decaying rates, b_{a} and b_{p}, respectively. The subscripts of a and p represent decaying rate estimated from amplitude and phase-lag plots, respectively, as mentioned by Nielsen (1990).

From Equation (36), the quantity of the aquifer parameter, $m = S/2k\phi_{\mathrm{w}}$, is proportional to the slope of a curve plotted with b^2 against frequency, ω. Fitted curves by the least square method for both b_{a}^2 and b_{p}^2 against frequencies from Nielson's measurements (1990) are shown in Figure 10.

Although field data show larger deviations from the fitted curves for longer periods, a good agreement between m_{a} and m_{p} is observed. The error between these two slopes is relatively small (5.2%). The discrepancy may be attributed to the effects of seepage face, heterogeneous and anisotropic properties of soils, etc.

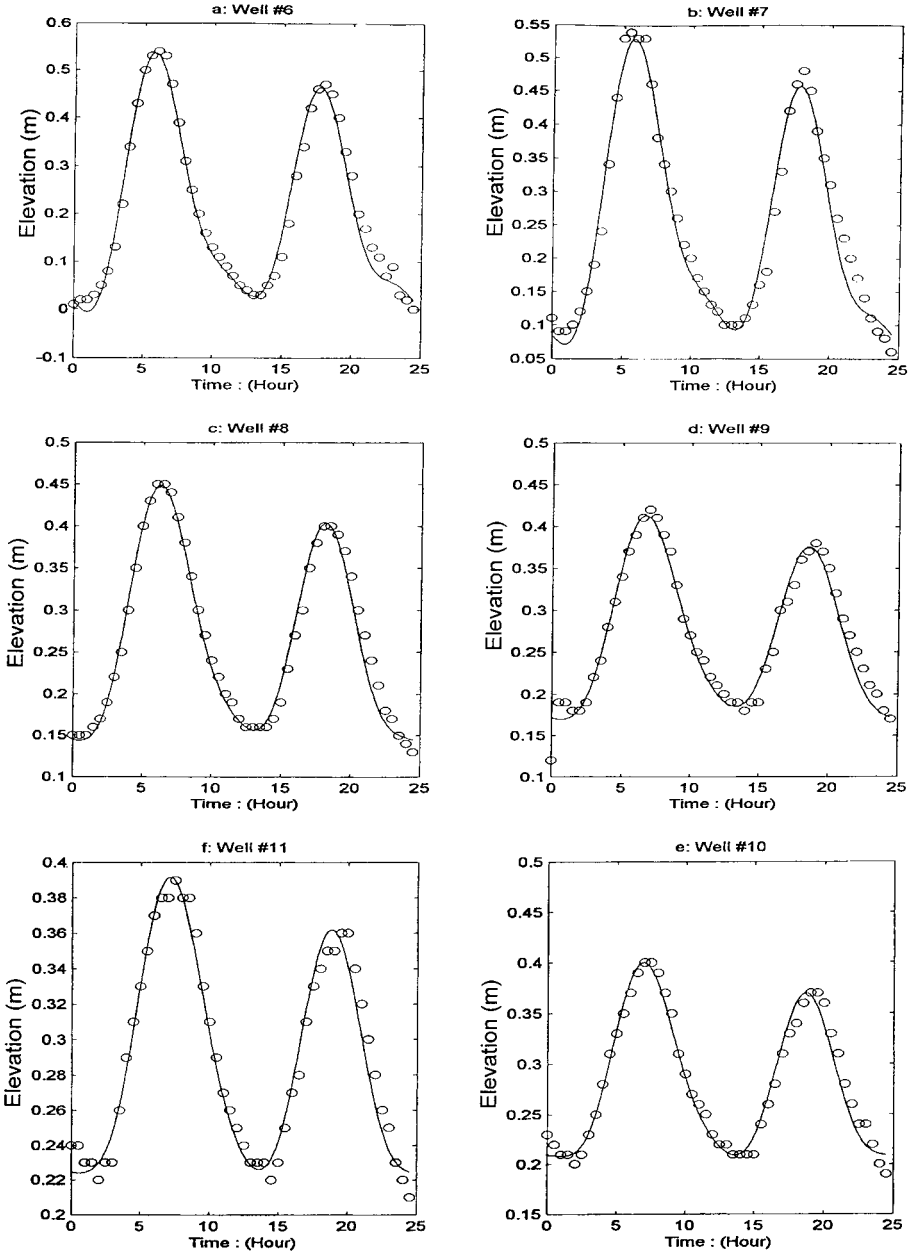

Figure 9. (a) ∼ (f) Five components fit of free-surface elevations at wells no. 6–10, 11. (Nielson, 1990).

4.4. ONE-DIMENSIONAL SHALLOW CONFINED INTERFACIAL FLOWS

In this section, the experiment made by Carr and van der Kamp (1969) at Nine Mile Creek of Prince Edward Island is reexamined (Figure 11). Tidal levels were

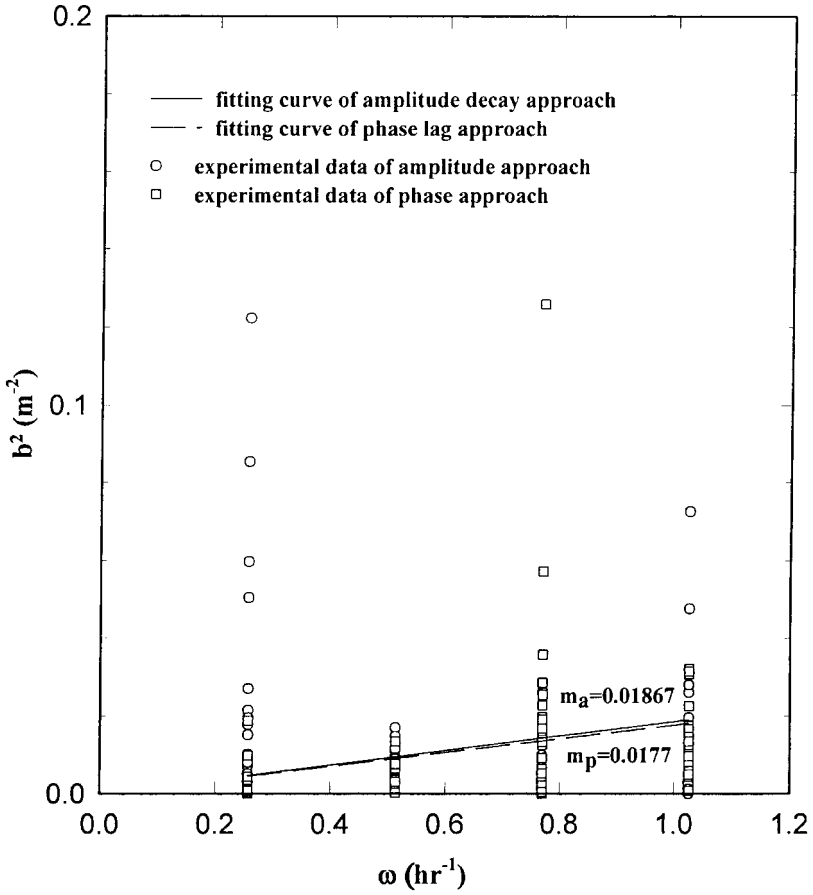

Figure 10. Least-square best fit of b^2/ω for an unconfined aquifer case.

measured at Charlottetown Habour. The water-level in well 3B located at Nine Mile Creek and 207 ft away from the coastline was measured. The coastline is defined by the mean sea level.

From results by Carr and van der Kamp (1969), m is computed to be 3.2858×10^{-4}h/m^2. On the other hand, tidal and well data are analyzed by using FFT to obtain the tidal spectrum and reconstruct fluctuation curves. Six major frequency and amplitude components are considered to fit the field data. With the same analyzing process in the previous section, m_a from amplitude-decay fitting and m_p from phase-lag fitting are 9.06×10^{-4} h/m^2 and 5.45×10^{-4} h/m^2, respectively. These two rates are different by a factor of about two, but are in the same order of magnitude. The physical parameters of a coastal aquifer should be revealed consistently from analyses of decaying amplitudes and lagging phases in observation wells.

Once the aquifer parameter, m, has been obtained by the tidal method illustrated in the previous section (Equation (39)), one can further use this parameter along

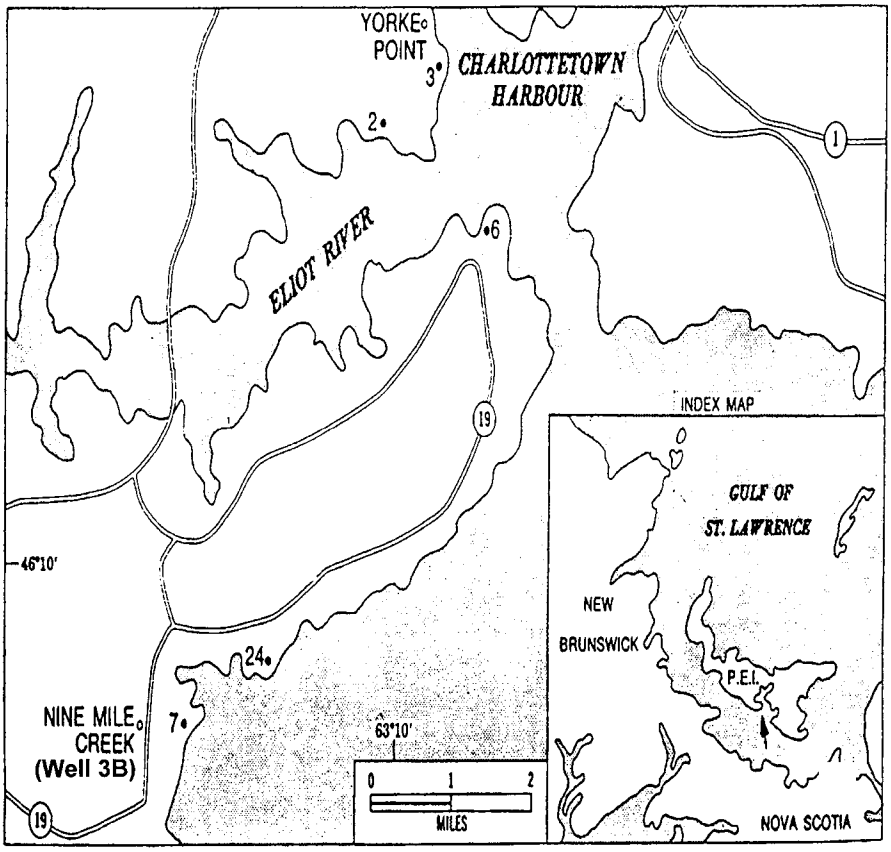

Figure 11. Location of observation well 3B on Nine Mile Creek and tidal gage at Charlottetown Harbour (after Carr and van der Kamp, 1969).

with tidal data to simulate the inland groundwater level at any location, such as 3B well. An illustration is presented by taking five tidal components. Amplitudes and frequencies of six tidal components are obtained from tidal spectrum. Mean sea level is represented by the elevation with zero frequency. With three values of m from Carr and van der Kamp's results (1969) and results from the previous paragraph (i.e. m_a, m_p), the different predicted water-levels at well 3B are calculated from Equation (39) and shown in Figure 12. Comparing the predicted water-levels with the field data at well 3B, it can be seen that the predicted curve with m_a is in good agreement with field data. The predicted curve with the parameter estimated by Carr and van der Kamp's results (1969) is much more deviated from field results. It seems to suggest that a good estimate of the aquifer parameter, m, may be obtained from the amplitude decaying rate of groundwater fluctuations due to tidal motions. Difficulty in correctly estimating phase lags may have caused errors of m_p.

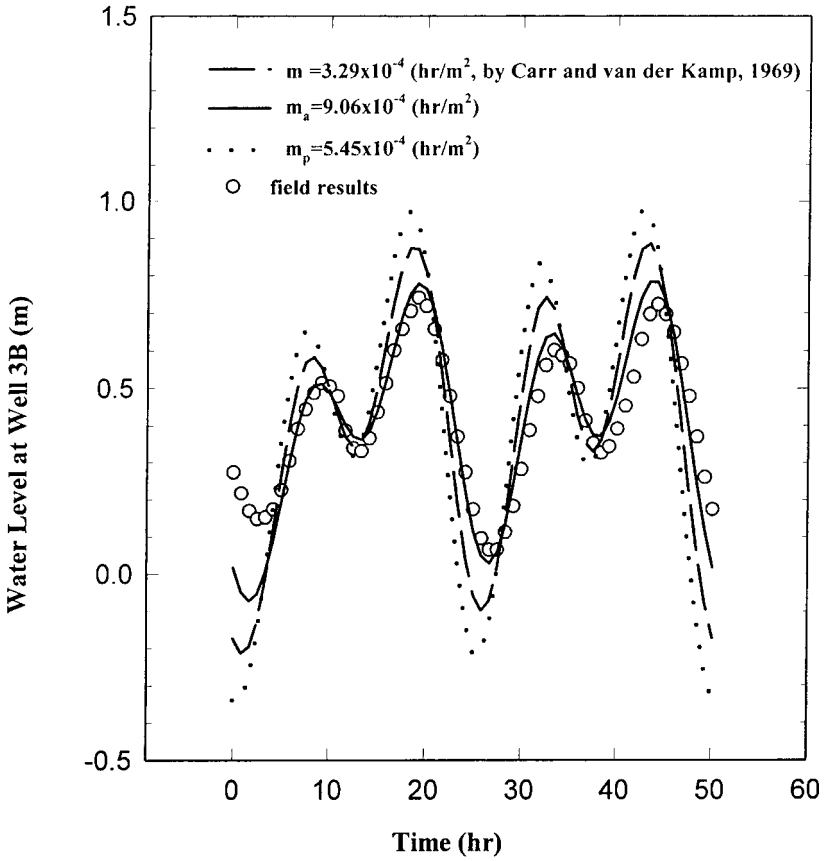

Figure 12. Comparison between computed levels and field data at well 3B.

5. Conclusions

Based on an approach of separating large- and small-time scale motions of groundwater fluctuations, a two-dimensional mathematical model was developed to evaluate tidal effects on groundwater motions. The model can describe the interfacial movement between freshwater and seawater in coastal aquifers. Approximate analytical solutions for a circular island and other one-dimensional cases of various flows were obtained. The amplitude of groundwater fluctuation decays with distance from the coastline, an aquifer parameter, m, and the tidal frequency. The phase lags of groundwater fluctuations due to tidal motions increase in a similar manner. Unfortunately no suitable data exist to verify the present two-dimensional analytical solutions. However, the present theory was verified for one-dimensional cases with experimental measurements for pure freshwater (Parlange *et al.*, 1984) and interfacial flows in an unconfined aquifer (Nielsen, 1990). The proposed method can estimate the aquifer parameter, m , from rates of amplitude decay and lags of phases in groundwater fluctuation due to tidal effects. Consistent

results of m, were obtained from amplitude decaying-rate and phase lags in Nielson's measurements (1990). Using the amplitude decaying-rate from groundwater fluctuations give a better estimate for m in Carr and van der Kamp's measurements (1969).

In real problems, the mixing layer between freshwater and saltwater and the effects of density variation should be considered. Present theory may be employed to estimate the layer thickness of groundwater density variation due to seawater intrusion.

Acknowledgements

The authors would like to thank reviewers for their comments and suggestions. Financial supports from National Science Council, Taiwan under contracts Nos. NSC-84-2611-E-002-011, NSC-85-2211-E-002-058, and NSC-86-2621-E-002-009 are appreciated.

References

Bear, J.: 1972, *Dynamics of Fluids in Porous Media*, Elsevier, New York.

Brutsaert, W. and Ibrahim, H. A.: 1966, Research note on the first and second linearization of the Boussinesq equation, *Geophys. J.R. Astron. Soc.* **11**, 549–554.

Carr, P. A. and van der Kamp, G. S.: 1969, Determining aquifer characteristics by the tidal method, *Water Resour. Res.* **5**(5), 1023–1031.

Ferris, J. G.: 1951, Cyclic fluctuations of water levels as a basis for determining aquifer transmissibility, *Intern. Assoc. Sci. Hydrology*, General Assembly, Blussels, Publ. 33, **2**, 305–318.

Knight, J. H.: 1981, Steady periodic flow through a rectangular dam, *Water Resour. Res.* **17**(4), 1222–1224.

Nutting, P. G.: 1930, Physical analysis of oil sands, *Bull. Am. Ass. Petrol. Geol.* **14**, 1337–1349.

Parlange, J. Y., Stagnitti, F., Starr, J. L. and Braddock, R.D.: 1984, Free surface flow in porous media and periodic solution of the shallow-flow approximation, *J. Hydrol.* **70**, 251–263.

Strack, O. D. L.:1989, *Groundwater Mechanics*, Prentice Hall, Englewood, NJ.